ACCEPTED MANUSCRIPT
DOI of the published work: https://doi.org/10.1016/j.engstruct.2022.114211
Engineering Structures, Volume 259, 15 May 2022, 114211

Topological Design of the Octahedron Tensegrity Family

Manuel Alejandro Fernández-Ruiz[a,*], Enrique Hernández-Montes[b], Luisa María Gil-Martín[c]

[a] Department of Industrial and Civil Engineering, Universidad de Cádiz (UCA). Campus Bahía de Algeciras, Avda. Ramón Puyol, s/n. 11201 Algeciras (Cádiz), Spain. manuelalejandro.fernandez@uca.es.
*Corresponding author

[b] Department of Structural Mechanics, University of Granada (UGR). Campus Universitario de Fuentenueva s/n. 18072 Granada, Spain. emontes@ugr.es.

[c] Department of Structural Mechanics, University of Granada (UGR). Campus Universitario de Fuentenueva s/n. 18072 Granada, Spain. mlgil@ugr.es.

Abstract

Tensegrity structures have developed greatly in recent years due to their unique mechanical and mathematical properties. In this work, the topology of the Octahedron family is presented. New tensegrity structures that belong to this family are defined based on their topology. As an example, the eleven-time-expanded octahedron is shown, a super-stable tensegrity formed by 12288 nodes, 6144 struts, and 24576 cables (the largest super-stable tensegrity reported in the literature in terms of number of nodes, cables, and struts so far). The values of the force:length ratios which satisfy the super-stability conditions have also been determined based on the topology of the Octahedron family. Consequently, the computational cost of the process of determining a suitable prestress state and its corresponding equilibrium shape (a process called form-finding) is significantly reduced. The members of the Octahedron family could have promising engineering and bioengineering applications.

Keywords: Tensegrity; Octahedron family; Analytical form-finding; Force density method.

1. Introduction

Tensegrity structures are spatial structures composed of pre-stressed pin-jointed compression and tension members (struts and cables, respectively) that are self-equilibrated. This type of structure has developed greatly in the last few decades due to their lightweight, ingenious forms, and their controllability and deployability. As a result, tensegrity structures are present in a wide range of scientific fields, such as civil engineering [1,2], robotics [3,4], aerospace [5] and biology [6,7]. In addition, they have promising applications as mechanical metamaterials [8,9].

The process used to find a self-equilibrated configuration (called a form-finding process) has a key role in the design of tensegrity structures. Tibert and Pellegrino [10] carried out a review of form-finding methods for tensegrity structures. The Force Density Method [11,12] (FDM) and the Dynamic Relaxation (DR) method [13] are the basis of most of these methods. Form-finding methods can be classified into numerical and analytical types. In the literature, there are several pieces of work about numerical form-finding methods [14–20]. On the other hand, only a few analytical form-finding methods can be found [21–23]. Analytical and numerical form-finding methods can be simplified if inherent symmetries and member types of the tensegrity are considered. The group representation theory is a powerful tool for symmetric tensegrities [24–27]. Non-gradient optimization methods used in structural engineering can be applied to tensegrity structures. Ant colony systems [28], genetic algorithms [29–32], and particle swarm optimization [33] are examples of these methods.

The FDM is based on the concept of force:length ratio or force density q [11,12], which

is defined as the ratio between the axial force and the length of each member of the tensegrity ($q > 0$ for cables and $q < 0$ for struts). The authors proposed in a previous work an analytical form-finding method of tensegrity structures based on FDM [21,34]. This method consists of finding a set of force:length ratios in a symbolic analysis that achieves an equilibrium shape of the tensegrity structures.

The DR method is based on a pseudo-dynamic process which treats tensegrity structures as a set of nodal masses and a set of elements with damping [35,36]. The DR method traces, step by step, in small time increments, and in accordance with Newton´s second law, the motion of each node of a structure until the structure, due to artificial damping, comes to rest in static equilibrium. There are other form-finding methods based on the stiffness matrix [37] and on geometric drawing [38].

Stability is another key aspect in the design of tensegrity structures. Super-stability is a stability criterion for tensegrity structures with by which the tensegrity is always stable regardless of the level of self-stress and material properties considered [39,40].

In the literature, tensegrity structures are mainly designed without considering member failure (such as yielding or buckling) [41]. However, there are some optimization methods that consider buckling constraints in order to avoid buckling [42]. The potential local buckling of compression members has not been considered in the present work.

The connectivity between the nodes of a tensegrity structure is an input of the form-finding problem. Tensegrity structures can be constructed by using purely geometric intuition based on geometric bodies [23,43,44] or by using topology [34,45,46]. A tensegrity family is a group of tensegrity structures that share a common connectivity pattern [34,47,48]. The Octahedron [34], the Z-Octahedron [47] and the X-Octahedron [48] families are examples of families of tensegrity structures found in the literature.

The Octahedron family [34] is composed by the octahedron, the expanded octahedron and the double-expanded octahedron.

The connectivity pattern presented in Fernández-Ruiz et al. [34] for the Octahedron family can only be applied for the definition of the three first members of the family. In this work, the topology of the Octahedron family is completely defined, obtaining all its members without any exceptions. As the first three members of the family are already known, the folding process from a member of the family to the previous one is studied. By doing so, the topology of the Octahedron family emerges clearly.

2. Analytical form-finding method for tensegrity structures

The equilibrium equations of a tensegrity with n nodes and m members can be formulated as [15,41]:

$$\begin{aligned} \mathbf{D}\,\mathbf{x} &= 0 \\ \mathbf{D}\,\mathbf{y} &= 0 \\ \mathbf{D}\,\mathbf{z} &= 0 \end{aligned} \tag{1}$$

where $\mathbf{D} = \mathbf{C}^{\mathrm{T}}\mathbf{Q}\mathbf{C}$ ($\in\Re^{n\times n}$) is the force density matrix and $\mathbf{x}$, $\mathbf{y}$, $\mathbf{z}$ ($\in\Re^{n}$) the nodal coordinate vectors. The symbol $[]^{\mathrm{T}}$ represents the transpose operation of a matrix or vector. The force:length ratio q of each member of the family and the connectivity matrix $\mathbf{C}$ are the inputs of the form-finding method. The connectivity matrix $\mathbf{C}$ ($\in\Re^{m\times n}$) shows the connectivity between the nodes of the tensegrity and it is constructed in the following way: if a general member j connects nodes i and k (with $i < k$), the ith and kth elements of the jth row of $\mathbf{C}$ are set to 1 and -1 respectively. The values of the force:length ratio of each member are collected in the vector $\mathbf{q} = (q_1, q_2, ..., q_m)$ ($\in\Re^{m}$), being $\mathbf{Q}$ the diagonal square matrix of vector $\mathbf{q}$.

A necessary condition for the development of a tensegrity with dimension d is that the rank deficiency of matrix $\mathbf{D}$ is at least $d + 1$ (non-degeneracy condition [16,21]). The

non-degeneracy condition is achieved imposing that the characteristic polynomial of **D** (see Eq. (2)) has $d + 1$ zero roots. By doing so, coefficients a_3, a_2, a_1 and a_0 of the characteristic polynomial must be zero in order to obtain a three-dimensional (3D) tensegrity. By construction of **D**, it is always singular and consequently coefficient a_0 is always 0. The system of equations in terms of the force:length ratios of the members of the 3D tensegrity shown in Eq. (3) is analytically solved in order to obtain a rank deficiency of matrix **D** of at least $d + 1$.

$$p(\lambda)=\lambda^n+a_{n-1}\lambda^{n-1}+\ldots+a_1\lambda+a_0 \tag{2}$$

$$\begin{aligned} a_3(q_1,\ldots,q_m) &= 0 \\ a_2(q_1,\ldots,q_m) &= 0 \\ a_1(q_1,\ldots,q_m) &= 0 \end{aligned} \tag{3}$$

A more detailed description of the analytical form-finding procedure used in this work can be seen in [21,34].

Matrix **D** can be directly formulated using the values of the force:length ratio of the members as:

$$\mathbf{D}_{ij} = \begin{cases} \sum_{k\in\Gamma} q_k & \text{for } i = j \\ -q_k & \text{if nodes } i \text{ and } j \text{ are connected by member } k \\ 0 & \text{otherwise} \end{cases} \tag{4}$$

With Γ as the set of members connected to the node i.

A super-stable tensegrity is always stable, regardless of material properties and prestress [39,40]. The super-stability conditions of tensegrity structures are as follows [39–41]:

1. The rank deficiency of the force density matrix **D** is exactly $d + 1$.
2. The force density matrix **D** is positive semi-definite.
3. The rank of the matrix **G** is $(d^2 + d)/2$.

An in-depth explanation on the geometry matrix **G** can be seen in [41]. The stability of tensegrity structures has been discussed in detail in [34,40,41]. All the full forms of the

members of the Octahedron family presented in this work fulfills all the super-stability conditions.

3. The Octahedron family

The Octahedron family (presented in Fernández-Ruiz et al. [34]) is composed of the octahedron, the expanded octahedron, and the double-expanded octahedron (see Figure 1). The members of the Octahedron family are sorted by the number of nodes in increasing order. Let p be the position of the tensegrity in the Octahedron family. Consequently, $p = 1$ for the octahedron (Figure 1.a), $p = 2$ for the expanded octahedron (Figure 1.b) and $p = 3$ for the double-expanded octahedron (Figure 1.c). The Octahedron family has the following properties [34]:

1. The members of the family are composed of rhombic cells.
2. Each member has twice the number of rhombic cells (and consequently, twice the number of nodes, cables and struts) of the previous member of the family.
3. Each member has as folded forms all the previous members of the family.
4. Rhombic cells are arranged in three groups.

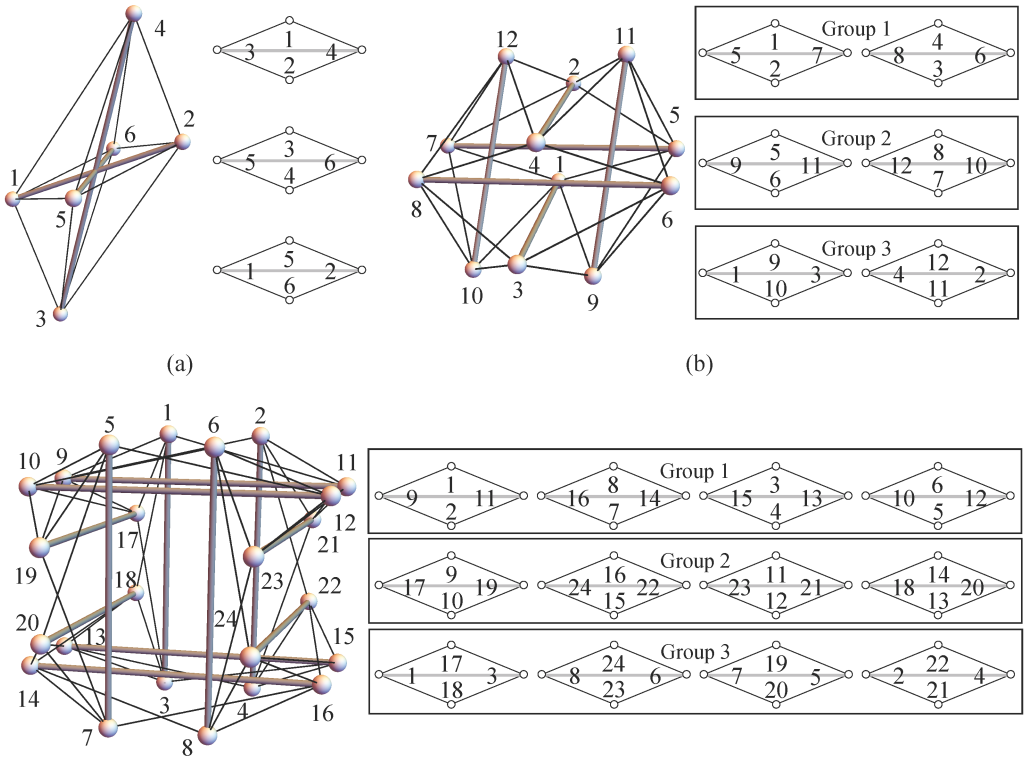

Figure 1. Octahedron (a), expanded octahedron (b) and double-expanded octahedron (c) and their corresponding rhombic cells. Thick gray and thin black lines correspond to struts and cables, respectively

The basic rhombic cell in the Octahedron family is formed by four nodes connected through four cables and one strut (see Figure 2). The top and bottom nodes are called principal nodes and, as can be seen in Figure 2, they are not connected by the strut. The two nodes connected by the strut are called secondary nodes. The numbering of the rhombic cells corresponding to the three first members of the Octahedron family (the ones known so far) have been obtained by following the connectivity pattern presented in Fernández-Ruiz et al.[34]. It is interesting to notice that the numbering of the nodes in a tensegrity is free, but the connectivity between them has to be kept unchanged.

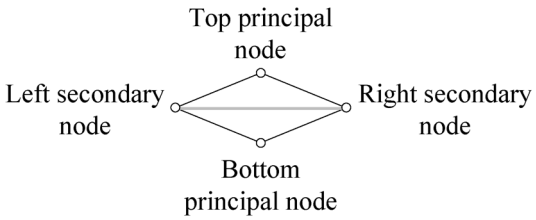

Figure 2. Elementary rhombic cell

Folded forms are tensegrity structures where some nodes in the equilibrium shape share the same position in the space [21]. On the other hand, full forms are tensegrity structures where all the nodes have different positions in the equilibrium configuration [21].

In the tensegrities of the Octahedron family shown in Figure 1, only two values of force:length ratio are considered: q_c for cables and q_b for bars/struts. The octahedron is the first (p = 1) and simplest member of the Octahedron family (see Figure 1.a). It is composed of 3 rhombic cells, 6 nodes, 3 struts, and 12 cables. The solution given by using the form-finding method [21,34] that leads to a super-stable equilibrium configuration is $q_b = -2q_c$. The second member of the Octahedron family (p = 2) is the expanded octahedron (see Figure 1.b). It is composed of 6 rhombic cells, 12 nodes, 6 struts, and 24 cables. The solutions to the form-finding problem are $q_b = -2q_c$ and $q_b = -3/2q_c$. The solution corresponding to $q_b = -3/2q_c$ is the super-stable full form of the expanded octahedron (see Figure 1.b). On the other hand, and according to the third property of the Octahedron family, the solution $q_b = -2q_c$ corresponds to the folded form of the expanded octahedron (which is the octahedron whose members are all duplicated). Finally, the third member of the Octahedron family (p = 3) is the double-expanded octahedron (see Figure 1.c). It is composed of 12 rhombic cells, 24 nodes, 12 struts, and 48 cables. In this case, the solutions to the form-finding problem are $q_b = -2q_c$, $q_b = -3/2q_c$ and $q_b = -4/3q_c$. The solution $q_b = -4/3q_c$ corresponds to the super-stable

full form of the double-expanded octahedron (see Figure 1.c) and the solutions $q_b = -3/2q_c$ and $q_b = -2q_c$ correspond to the folded forms of the double-expanded octahedron (the expanded octahedron whose members are all duplicated and the octahedron whose members are all quadruplicated, respectively). These results indicate that, at the end of the folding process of a member of the Octahedron family, all the struts (and consequently, all the rhombic cells) will overlap each other in the three struts of the first member (the octahedron). For this reason, the cells of all the members of the family always form three groups, which duplicate the number of cells in each expansion. For example: the expanded octahedron has two rhombic cells per group, the double-expanded octahedron has four rhombic cells per group (see Figure 1), and so on.

4. Topology of the Octahedron family

The folding processes from the expanded octahedron to the octahedron and from the double-expanded octahedron to the expanded octahedron are analyzed in detail in order to define the topology of the Octahedron family.

Figure 3.a shows the equilibrium configuration of the expanded octahedron depicted in Figure 1.b with $q_b = -2q_c$. It is an octahedron whose nodes, struts, and cables are all duplicated. This is because the octahedron is a folded form of the expanded octahedron (or, from another perspective, the expanded octahedron is the expansion of the octahedron). For this reason, there are pairs of nodes that have the same position in the space (see the numbering of nodes in Figure 3.a). It can be seen that struts 5 – 7 and 8 – 6 overlap because nodes 5 – 8 and 7 – 6 have the same coordinates in the space, respectively. Consequently, the struts 5 – 7 and 8 – 6 of Figure 1.b (that are both in group 1) come from the expansion of the strut 3 – 4 of Figure 1.a. Figure 3.b shows the overlapped rhombic cells of the expanded octahedron. Each pair of nodes is composed

of two nodes that belong to different rhombic cells (italic and bold numbers, respectively). This distinction has been made based on the rhombic cells shown in Figure 1.b. In Figure 3.c the overlapped rhombic cells are shown separately. Obviously, the rhombic cells shown in Figure 3.c coincide with the ones shown in Figure 1.b.

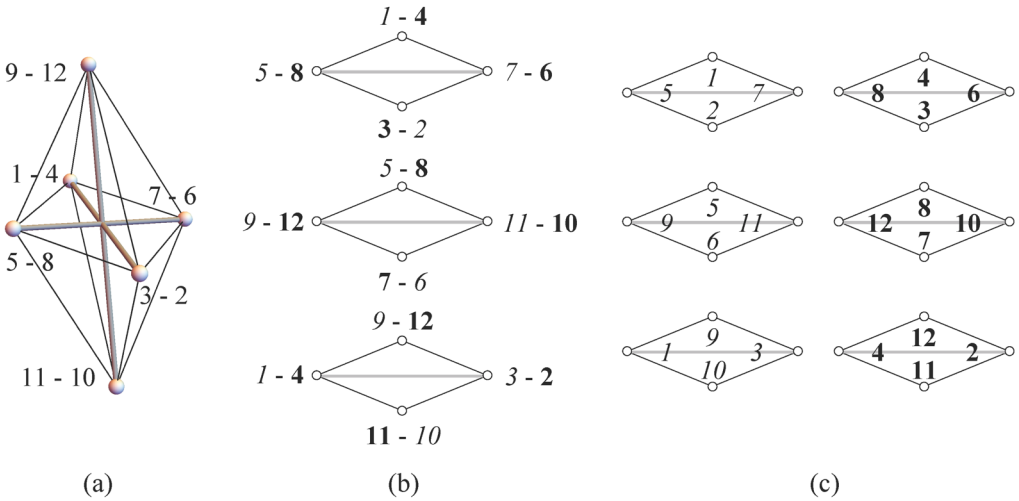

(a) (b) (c)

Figure 3. Expanded octahedron with $q_b = -2q_c$ (a), overlapped rhombic cells (b) and rhombic cells (c). Thick gray and thin black lines correspond to struts and cables, respectively.

Figure 4.a shows the equilibrium configuration of the double-expanded octahedron depicted in Figure 1.c with $q_b = -3/2q_c$. It corresponds to an expanded octahedron whose nodes, struts, and cables are all duplicated (see the numbering of nodes of Figure 4.a). In this case, 6 overlapped rhombic cells are shown in Figure 4.b, resulting in 12 rhombic cells (see Figure 4.c). As expected, the rhombic cells in Figure 4.c coincide with the ones in Figure 1.c.

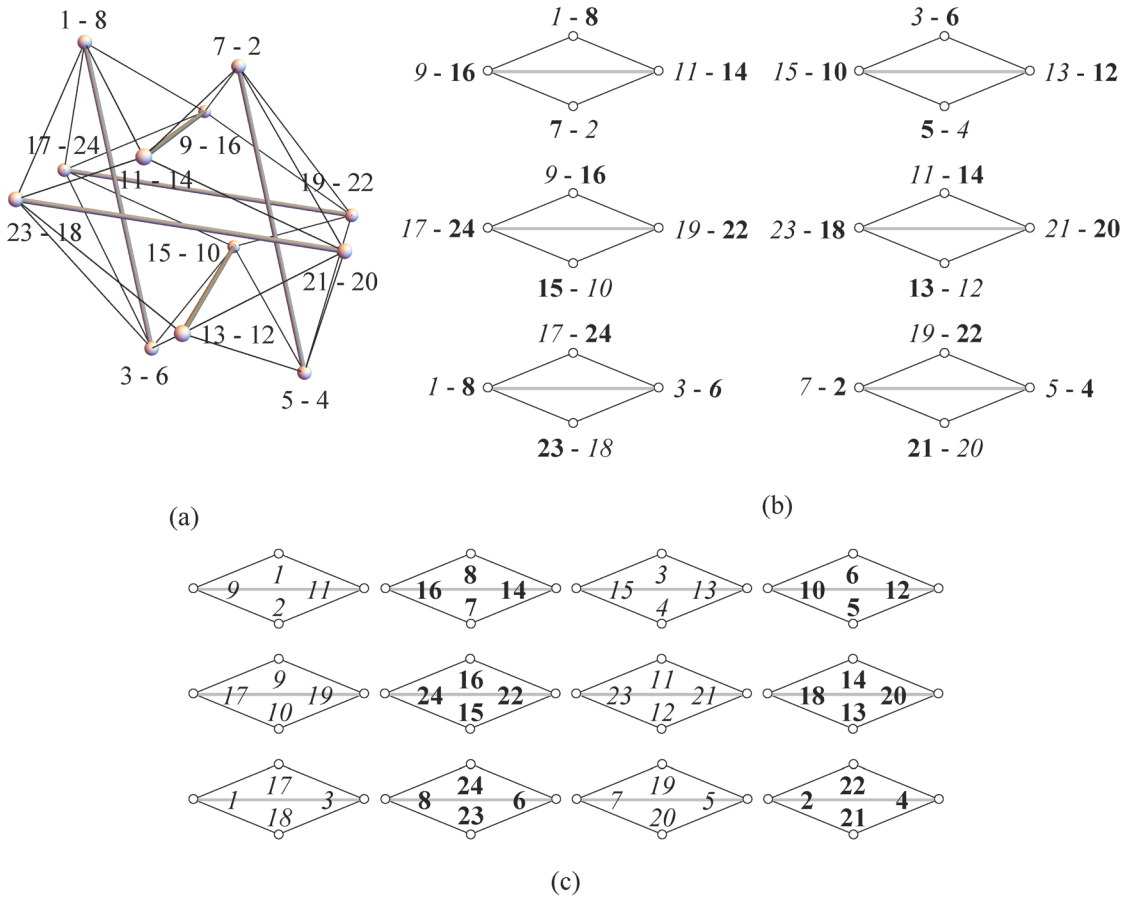

Figure 4. Double-expanded octahedron with $q_b = -3/2q_c$ (a), overlapped rhombic cells (b) and rhombic cells (c). Thick gray and thin black lines correspond to struts and cables, respectively.

Let us consider Figure 3 and 4 from another point of view. Instead of studying the folding of a member of the family to the previous one, at this point, the expansion of a member of the family to the subsequent one is considered. Based on Figure 3 and 4, the rhombic cells of ALL the members of the Octahedron family can be obtained by following these steps (with the exception of the octahedron, because it is not the expansion of a previous member of the family):

1. Draw a $3 \times 2^{(p-2)}$ matrix of overlapped rhombic cells.
2. Number all the pairs of principal nodes of each rhombic cell consecutively (see Figure 5.a).
3. Number the secondary nodes as the principal nodes of the following group of

rhombic cells in a consecutive order from left to right and from top to bottom (see Figure 5.b). Note that the groups of rhombic cells form a closed loop, so group 1 comes after group 3 (see the detail in Figure 5.b).

4. Separate the overlapped rhombic cells so that one rhombic cell is defined by the top-left principal node, by both the secondary nodes on the left and by the bottom-right principal node (see the squared numbers in Figure 5.b). The other rhombic cell is defined by the rest of nodes.

The example shown in Figure 5 corresponds to the expansion of the expanded octahedron to the double-expanded octahedron. The way in which this has been determined is novel: from the expansion of the previous member of the family (expanded octahedron in this case) by following the topology of the Octahedron family.

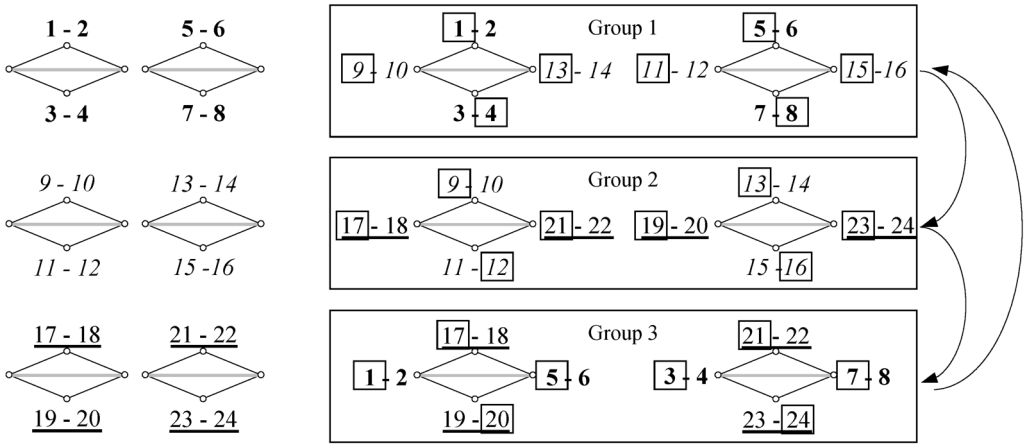

Figure 5. Expansion from the expanded octahedron to the double-expanded octahedron

5. New members of the Octahedron family

Let us apply the topology of the Octahedron family to determine the fourth member: the triple-expanded octahedron ($p = 4$). The 24 rhombic cells of the triple-expanded octahedron have been defined following the steps described in Section 4. The solutions

of the form-finding problem are $q_b = -2q_c$, $q_b = -3/2q_c$, $q_b = -4/3q_c$, and $q_b = -5/4q_c$. The solution $q_b = -5/4q_c$ corresponds to the super-stable, full form of the triple-expanded octahedron (see Figure 6), which is composed of 24 rhombic cells, 48 nodes, 24 struts, and 96 cables. It can be proved that the solutions $q_b = -4/3q_c$, $q_b = -3/2q_c$, and $q_b = -2q_c$ correspond to the folded forms of the triple-expanded octahedron: the double-expanded octahedron, the expanded octahedron, and the octahedron, respectively. This confirms that this tensegrity belongs to the Octahedron family.

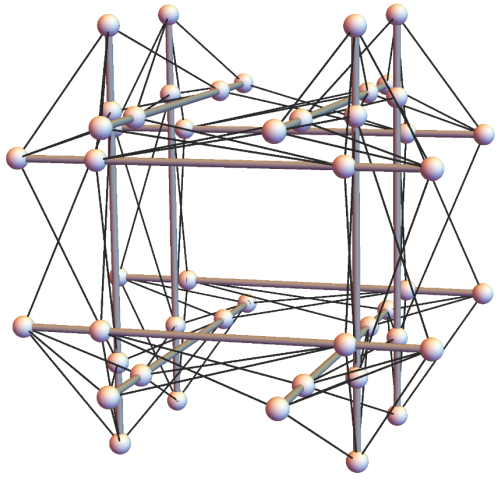

Figure 6. Triple-expanded octahedron

It can be concluded that this newly presented topology represents a general pattern that extends the connectivity pattern previously defined in Fernández-Ruiz et al. [34]. Moreover, the topology of the Octahedron family can be easily programmed in order to define the numbering of the rhombic cells of subsequent members.

For the sake of clarity and without loss of generality, in all the tensegrities shown in this work, only two force:length ratios have been considered (q_c for cables and q_b for bars/struts). The analytical form-finding method proposed in [21,34] has been used to compute the force:length ratios that lead to an equilibrium configuration of the

tensegrity.

The solutions to the form-finding problem of the full forms of the members of the Octahedron family are $q_b = -2q_c$ for the octahedron, $q_b = -3/2q_c$ for the expanded octahedron, $q_b = -4/3q_c$ for the double-expanded octahedron and $q_b = -5/4q_c$ for the triple-expanded octahedron (all of which are super-stable tensegrities). It can be seen that the force:length ratios of the tensegrities of the Octahedron family follow the mathematical sequence shown in Eq. (5) and depicted in Figure 7.

$$\frac{q_b}{q_c} = -\frac{p+1}{p} \tag{5}$$

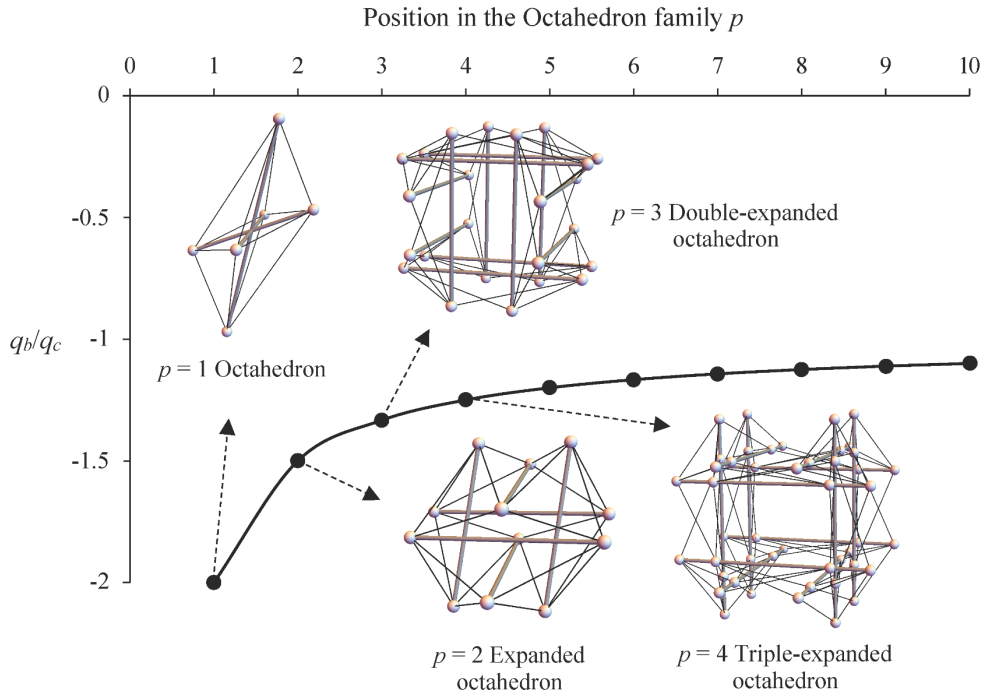

Figure 7. Sequence of solutions of q_b/q_c of the Octahedron family shown in Eq. (5)

Figure 8 shows the equilibrium configurations of the five-time-expanded octahedron, six-time-expanded octahedron, nine-time-expanded octahedron, and eleven-time-expanded octahedron (all of them super-stable). It should be highlighted that the eleven-time-expanded octahedron shown in Figure 8.d is a super-stable tensegrity formed by

12288 nodes, 6144 struts and 24576 cables. As far as the authors know, a super-stable tensegrity with such a high number of nodes, struts, and cables has not been reported in the literature. Moreover, the procedure presented in this paper allows an endless number of new super-stable tensegrities based on the topology of the Octahedron family to be obtained. Finally, it has been proved that the sequence shown in Eq. (5) is valid for all the members of the Octahedron family presented in this work. The highest computation cost of the form-finding method is the computation of the analytical solution of the system of equations shown in Eq. (3). The sequence of solutions of q_b/q_c followed by the members of the Octahedron family means that this step can be avoided. Consequently, the form-finding process of the members of the Octahedron family is reduced to a calculation of the eigenvectors of **D** (Eq. (1)).

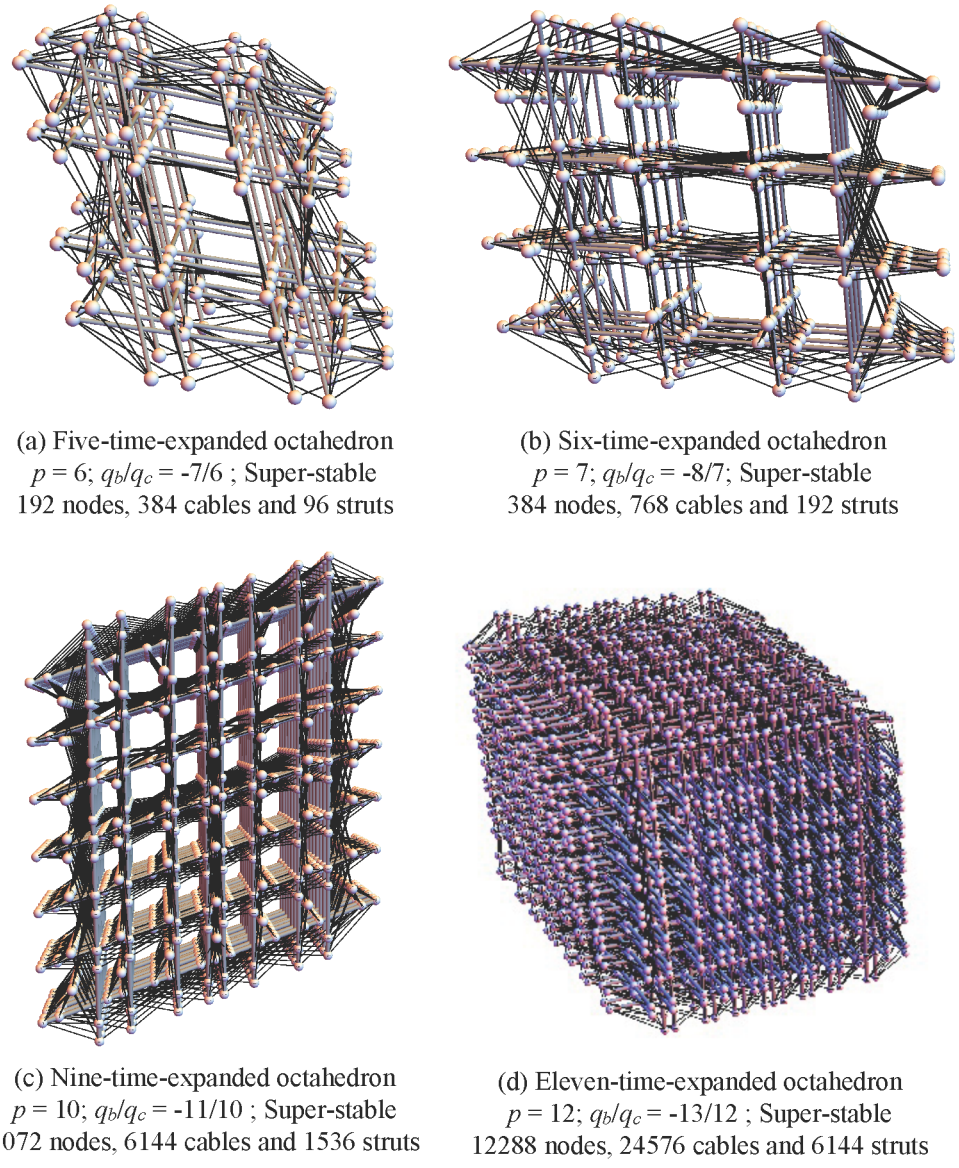

(a) Five-time-expanded octahedron
$p = 6$; $q_b/q_c = -7/6$; Super-stable
192 nodes, 384 cables and 96 struts

(b) Six-time-expanded octahedron
$p = 7$; $q_b/q_c = -8/7$; Super-stable
384 nodes, 768 cables and 192 struts

(c) Nine-time-expanded octahedron
$p = 10$; $q_b/q_c = -11/10$; Super-stable
3072 nodes, 6144 cables and 1536 struts

(d) Eleven-time-expanded octahedron
$p = 12$; $q_b/q_c = -13/12$; Super-stable
12288 nodes, 24576 cables and 6144 struts

Figure 8. Five-time-expanded octahedron (a), six-time-expanded octahedron (b), nine-time-expanded octahedron (c), and eleven-time-expanded octahedron (d)

Tensegrities shown in Figure 8 have a quasiregular square honeycomb shape. Honeycomb materials have high strength, specific stiffness, and energy absorption efficiency [49–51] and they are widely observed in natural materials [52]. Tensegrity metamaterials can be used in impact protection systems, energy dissipation systems, and in adaptive load-bearing structures [9,53]. In view of the cubic symmetry of the members of the Octahedron family, group representation theory can be used to simplify

the form-finding process [27]. Besides this, some members of the Octahedron family, such as the double and triple-expanded octahedrons, can be considered as tensegrity modules for the design of pedestrian bridges [54]. Due to these characteristics, the members of the Octahedron family such as the eleven-time-expanded octahedron could have promising engineering and bioengineering applications.

6. Conclusions

The topology of the Octahedron family is completely developed. Up to now, only three members of the Octahedron family were known: the octahedron, the expanded octahedron and the double-expanded octahedron. The folding process from a member of the family to the previous one has been analyzed in order to define the topology of the family. The topology presented in this work has been adapted to the definition of all the members of the Octahedron family. An analytical form-finding method has been used to compute the equilibrium configuration of the studied tensegrities. It is remarkable that no nodal coordinates or nodal connectivity are required as initial input data, only the position of the tensegrity in the Octahedron family p. The ratio between the force:length ratio of struts and cables (q_b/q_c) that leads to a super-stable equilibrium configuration of the members of the family follows a mathematical sequence that depends on p. Therefore, the computation cost of the analytical form-finding method is significantly diminished (it is reduced to the calculation of the eigenvectors of the force density matrix of the tensegrity). The eleven-time-expanded octahedron is depicted to illustrate the potential of the Octahedron family. This super-stable tensegrity is formed by 12288 nodes, 6144 struts, and 24576 cables, and it is, the largest super-stable tensegrity reported in the literature (in terms of number of nodes, cables, and struts) so far. By applying the procedure presented in this paper, subsequent members of the Octahedron

family can be defined. Finally, due to their quasiregular honeycomb shape, the members of the Octahedron family could have promising engineering and bioengineering applications.

References

[1] Veuve N, Dalil Safaei S, Smith IFC. Active control for mid-span connection of a deployable tensegrity footbridge. Eng Struct 2016;112:245–55. doi:10.1016/j.engstruct.2016.01.011.

[2] Feng Y, Yuan X, Samy A. Analysis of new wave-curved tensegrity dome. Eng Struct 2022;250:113408. doi:10.1016/j.engstruct.2021.113408.

[3] Liu S, Li Q, Wang P, Guo F. Kinematic and static analysis of a novel tensegrity robot. Mech Mach Theory 2020;149:103788. doi:10.1016/j.mechmachtheory.2020.103788.

[4] Wang Z, Li K, He Q, Cai S. A light-powered ultralight tensegrity robot with high deformability and load capacity. Adv Mater 2019;31:1806849. doi:https://doi.org/10.1002/adma.201806849.

[5] Chen M, Goyal R, Majji M, Skelton RE. Design and analysis of a growable artificial gravity space habitat. Aerosp Sci Technol 2020;106:106147. doi:10.1016/j.ast.2020.106147.

[6] Ingber DE. The Architecture of Life. Sci Am 1998;278:48–57.

[7] Scarr G. Biotensegrity: The structural basis of life. Handspring Publishing: 2014.

[8] Yin X, Gao ZY, Zhang S, Zhang LY, Xu GK. Truncated regular octahedral tensegrity-based mechanical metamaterial with tunable and programmable Poisson's ratio. Int J Mech Sci 2020;167:105285. doi:10.1016/j.ijmecsci.2019.105285.

[9] Ma Y, Zhang Q, Dobah Y, Scarpa F, Fraternali F, Skelton RE, et al. Meta-tensegrity: Design of a tensegrity prism with metal rubber. Compos Struct 2018;206:644–57. doi:10.1016/j.compstruct.2018.08.067.

[10] Tibert AG, Pellegrino S. Review of Form-Finding Methods for Tensegrity Structures. Int J Sp Struct 2003;18:209–23. doi:10.1260/026635103322987940.

[11] Linkwitz K, Schek HJ. Einige Bemerkungen zur Berechnung von vorgespannten Seilnetzkonstruktionen. Ingenieur-Archiv 1971;40:145–58. doi:10.1007/BF00532146.

[12] Schek HJ. The force density method for form-finding and computation of general networks. Comput Methods Appl Mech Eng 1974;3:115–34. doi:10.1016/0045-7825(74)90045-0.

[13] Otter JRH. Computations for prestressed concrete reactor pressure vessels using dynamic relaxation. Nucl Struct Eng 1965;1:61–75. doi:10.1016/0369-5816(65)90097-9.

[14] Yuan S, Zhu W. Optimal self-stress determination of tensegrity structures. Eng Struct 2021;238:112003. doi:10.1016/j.engstruct.2021.112003.

[15] Tran HC, Lee J. Advanced form-finding of tensegrity structures. Comput Struct 2010;88:237–46. doi:10.1016/j.compstruc.2009.10.006.

[16] Zhang JY, Ohsaki M. Adaptive force density method for form-finding problem of tensegrity structures. Int J Solids Struct 2006;43:5658–73. doi:10.1016/j.ijsolstr.2005.10.011.

[17] Estrada GG, Bungartz H-J, Mohrdieck C. Numerical form-finding of tensegrity structures. Int J Solids Struct 2006;43:6855–68.

[18] Cai J, Feng J. Form-finding of tensegrity structures using an optimization method. Eng Struct 2015;104:126–32. doi:10.1016/j.engstruct.2015.09.028.

[19] Tran HC, Lee J. Form-finding of tensegrity structures using double singular value decomposition. Eng Comput 2011;29:71–86. doi:10.1007/s00366-011-0245-7.

[20] Tran HC, Lee J. Form-finding of tensegrity structures with multiple states of self-stress. Acta Mech 2011;222:131–47. doi:10.1007/s00707-011-0524-9.

[21] Hernández-Montes E, Fernández-Ruiz MA, Gil-Martín LM, Merino L, Jara P. Full and folded forms: a compact review of the formulation of tensegrity structures. Math Mech Solids 2018;23:944–9. doi:10.1177/1081286517697372.

[22] Vassart N, Motro R. Multiparameted form-finding method: application to tensegrity systems. Int J Sp Struct 1999;14:89–104.

[23] Zhang LY, Li Y, Cao YP, Feng XQ. A unified solution for self-equilibrium and super-stability of rhombic truncated regular polyhedral tensegrities. Int J Solids Struct 2013;50:234–45. doi:10.1016/j.ijsolstr.2012.09.024.

[24] Chen Y, Feng J. Generalized eigenvalue analysis of symmetric prestressed structures using group theory. J Comput Civ Eng 2012;26:488–97. doi:10.1061/(ASCE)CP.1943-5487.0000151.

[25] Chen Y, Sun Q, Feng J. Improved Form-Finding of Tensegrity Structures Using Blocks of Symmetry-Adapted Force Density Matrix. J Struct Eng 2018;144:04018174. doi:10.1061/(asce)st.1943-541x.0002172.

[26] Zhang JY, Ohsaki M, Tsuura F. Self-equilibrium and super-stability of truncated regular hexahedral and octahedral tensegrity structures. Int J Solids Struct 2019;161:182–92. doi:10.1016/j.ijsolstr.2018.11.017.

[27] Zhang JY, Guest SD, Ohsaki M. Symmetric prismatic tensegrity structures. Part II: Symmetry-adapted formulations. Int J Solids Struct 2009;46:15–30. doi:10.1016/j.ijsolstr.2008.07.035.

[28] Chen Y, Feng J, Wu Y. Novel Form-Finding of Tensegrity Structures Using Ant Colony Systems. J Mech Robot 2012;4:1–7. doi:10.1115/1.4006656.

[29] Lee S, Gan BS, Lee J. A fully automatic group selection for form-finding process of truncated tetrahedral tensegrity structures via a double-loop genetic algorithm. Compos Part B 2016;106:308–15. doi:10.1016/j.compositesb.2016.09.018.

[30] Bel Hadj Ali N, Rhode-Barbarigos L, Pascual Albi AA, Smith IFC. Design optimization and dynamic analysis of a tensegrity-based footbridge. Eng Struct 2010;32:3650–9. doi:10.1016/j.engstruct.2010.08.009.

[31] Lee S, Lee J. Advanced automatic grouping for form-finding of tensegrity structures. Struct Multidiscip Optim 2017;55:959–68. doi:10.1007/s00158-016-1549-4.

[32] Do DTT, Lee S, Lee J. A modified differential evolution algorithm for tensegrity structures. Compos Struct 2016;158:11–9. doi:10.1016/j.compstruct.2016.08.039.

[33] Yildiz K, Lesieutre GA. Sizing and prestress optimization of Class-2 tensegrity structures for space boom applications. Eng Comput 2020. doi:10.1007/s00366-020-01111-x.

[34] Fernández-Ruiz MA, Hernández-Montes E, Carbonell-Márquez JF, Gil-Martín LM. Octahedron family: The double-expanded octahedron tensegrity. Int J Solids Struct 2019;165:1–13. doi:10.1016/j.ijsolstr.2019.01.017.

[35] Adriaenssens SML, Barnes MR. Tensegrity spline beam and grid shell structures. Eng Struct 2001;23:29–36. doi:10.1016/S0141-0296(00)00019-5.

[36] Zhang J, Ohsaki M. Form-finding of complex tengrity structures by dynamic relaxation method. J Struct Constr Eng 2016;81:71–7. doi:10.3130/aijs.81.71.

[37] Zhang L-Y, Li Y, Cao Y-P, Feng X-Q. Stiffness matrix based form-finding method of tensegrity structures. Eng Struct 2014;58:36–48.

427 doi:10.1016/j.engstruct.2013.10.014.
428 [38] Shang R, Zhao Y, Yin Z. Geometric Drawing Method for Form-finding and
429 Force-finding to Triangular Prism Tensegrity with End Surfaces not Paralleled. J
430 Phys Conf Ser 2020;1624. doi:10.1088/1742-6596/1624/5/052012.
431 [39] Connelly R. Tensegrity structures. Why are they stable? In: Thorpe MF, Duxbury
432 PM, editors. Rigidity theory Appl., Kluwer Academic / Plenum Publishers; 1998,
433 p. 47–54.
434 [40] Zhang JY, Ohsaki M. Stability conditions for tensegrity structures. Int J Solids
435 Struct 2007;44:3875–86. doi:10.1016/j.ijsolstr.2006.10.027.
436 [41] Zhang JY, Ohsaki M. Tensegrity Structures. Form, Stability, and Symmetry.
437 Springer; 2015.
438 [42] Xu X, Wang Y, Luo Y, Hu D. Topology Optimization of Tensegrity Structures
439 Considering Buckling Constraints. J Struct Eng 2018;144:04018173.
440 doi:10.1061/(asce)st.1943-541x.0002156.
441 [43] Li Y, Feng XQ, Cao YP, Gao H. Constructing tensegrity structures from one-bar
442 elementary cells. Proc R Soc A Math Phys Eng Sci 2010;466:45–61.
443 doi:10.1098/rspa.2009.0260.
444 [44] Zhang LY, Li Y, Cao YP, Feng XQ, Gao H. Self-equilibrium and super-stability
445 of truncated regular polyhedral tensegrity structures: A unified analytical
446 solution. Proc R Soc A Math Phys Eng Sci 2012;468:3323–47.
447 doi:10.1098/rspa.2012.0260.
448 [45] Lee S, Lee J. A novel method for topology design of tensegrity structures.
449 Compos Struct 2016;152:11–9. doi:10.1016/j.compstruct.2016.05.009.
450 [46] Kanno Y. Topology optimization of tensegrity structures under self-weight loads.
451 J Oper Res Soc Japan 2012;55:125–45.

[47] Fernández-Ruiz MA, Hernández-Montes E, Gil-Martín LM. The Z-octahedron family: A new tensegrity family. Eng Struct 2020;222:111151. doi:10.1016/j.engstruct.2020.111151.

[48] Fernández-Ruiz MA, Hernández-Montes E, Gil-Martín LM. The Octahedron family as a source of tensegrity families: The X-Octahedron family. Int J Solids Struct 2021;208–209:1–12. doi:10.1016/j.ijsolstr.2020.10.019.

[49] Jiang W, Yan L, Ma H, Fan Y, Wang J, Feng M, et al. Electromagnetic wave absorption and compressive behavior of a three-dimensional metamaterial absorber based on 3D printed honeycomb. Sci Rep 2018;8:1–7. doi:10.1038/s41598-018-23286-6.

[50] Tao Y, Li W, Wei K, Duan S, Wen W, Chen L, et al. Mechanical properties and energy absorption of 3D printed square hierarchical honeycombs under in-plane axial compression. Compos Part B Eng 2019;176:107219. doi:10.1016/j.compositesb.2019.107219.

[51] Wang Z. Recent advances in novel metallic honeycomb structure. Compos Part B Eng 2019;166:731–41. doi:10.1016/j.compositesb.2019.02.011.

[52] Zhang Q, Yang X, Li P, Huang G, Feng S, Shen C, et al. Bioinspired engineering of honeycomb structure - Using nature to inspire human innovation. Prog Mater Sci 2015;74:332–400. doi:10.1016/j.pmatsci.2015.05.001.

[53] Bauer J, Kraus JA, Crook C, Rimoli JJ, Valdevit L. Tensegrity Metamaterials: Toward Failure-Resistant Engineering Systems through Delocalized Deformation. Adv Mater 2021;33:1–9. doi:10.1002/adma.202005647.

[54] Rhode-Barbarigos L, Hadj Ali NB, Motro R, Smith IFC. Designing tensegrity modules for pedestrian bridges. Eng Struct 2010;32:1158–67. doi:10.1016/j.engstruct.2009.12.042.